

THESIS

LIPID RAFT SIGNALING IN COFILIN-ACTIN ROD FORMATION INDUCED
BY AMYLOID- β AND TNF α .

Submitted by

Jianjie Mi

Department of Biochemistry and Molecular Biology

In partial fulfillment of the requirements

For the Degree of Master of Science

Colorado State University

Fort Collins, Colorado

Fall 2012

Master's Committee:

Advisor: James R. Bamberg

ChaoPing Chen

Kathryn M. Partin

ABSTRACT

LIPID RAFT SIGNALING IN COFILIN-ACTIN ROD FORMATION INDUCED BY AMYLOID- β AND TNF α .

Rod-like inclusions (rods), composed of actin saturated with cofilin, are induced in neurons by energetic and oxidative stresses, excitotoxic levels of glutamate, and amyloid beta treatment. Cofilin is an F-actin assembly regulatory protein critical to various actin-dependent processes, such as cytokinesis, cell migration, and neurite formation. Overexpression or hyperactivation (excessive dephosphorylation) of cofilin coupled with its oxidation can lead to formation of rods. Rods represent a likely mechanism to explain the synaptic loss associated with early stages of Alzheimer's disease (AD) and thus represent a novel target for therapeutic intervention.

In live neurons, the study of cofilin-actin rod formation induced by specific mediators of stress has been limited because overexpression of fluorescent protein-tagged wild type (WT) cofilin results in formation of considerable numbers of spontaneous rods. A fluorescent cofilin mutant that could incorporate into induced rods but form no spontaneous rods even when overexpressed would offer a useful alternative for live-cell imaging. The R21Q mutant cofilin-RFP has been reported to not induce rods when overexpressed but incorporates into rods containing endogenous cofilin, thus serving as a rod marker in live cells. Here we show that expression of WT cofilin driven by promoters that result in a high or moderate steady-state level of

exogenous protein produces a significant number of spontaneous rods, three to four fold over controls. However, R21Q cofilin-RFP expressed behind these same promoters will only incorporate into rods formed from endogenous protein, but not enhance spontaneous rod, even when accompanied by the photo stress induced by microscopic observation. Using the R21Q cofilin- RFP to measure rod formation, we then showed that the proinflammatory cytokine (TNF α) induced about a 3 fold increase in rod formation over untreated controls quantified either as the percent of neurons with rods (percent rod index) or as the number of rods per field (number rod index). Amyloid beta dimer/trimer (A β d/t) induced about a 2.5 fold increase over controls in the percent of neurons with rods, and close to a 2 fold increase in the number of rods per field. To determine the fidelity of the R21Q cofilin-RFP in labeling all of the rods, we induced rods in control infected or R21Q cofilin-RFP expressing neurons with ATP depletion for 30 min, or with either A β d/t (250 pM) or TNF α (50 ng/ml; 2.9 nM) for 24 h. Neurons were fixed and immunostained with a primary antibody for cofilin and an Alexa 647 nm-labeled secondary antibody. The percent of rods in RFP expressing cells that co-labeled with mRFP and Alexa 647 were then quantified. Although 100% of rods induced by ATP depletion co-labeled, surprisingly only 48% of the rods induced by TNF α co-labeled, similar to A β d/t treatment. The reasons for this are not clear but taken together, our results demonstrate that R21Q cofilin-RFP can be used for a live cell marker for following induced rod formation but not as a quantitative measure of the total rod response.

Induction of cofilin-actin rods by amyloid beta and TNF α is mediated by the cellular prion protein, a component of lipid raft domains which can signal to activate NADPH oxidase. Lipid rafts are cholesterol/sphingolipid enriched detergent resistant membrane domains in which many membrane receptors associate. Rafts can be visualized with an Alexa labeled cholera toxin B subunit which binds to G_{M1} ganglioside. Here we used neurons expressing R21Q cofilin-RFP to determine if rod formation is associated with coalesced lipid raft domains and if the coalesced lipid rafts form before or after rods are visible. In the three rods we visualized forming during the period in which lipid rafts were labeled we saw no lipid raft coalescence at sites of the newly formed rods. If we looked at the total R21Q cofilin-RFP labeled rods, about 45% of them co-localize with enlarged lipid raft domains. Thus results suggest that rods may bring about the reorganization of the membrane raft domains, although more data are required to make a definitive conclusion.

ACKNOWLEDGMENTS

I would especially like to thank my advisor, Dr. James Bamberg for his guidance and direction. I would also give thanks to the members of my committee, Dr. Chaoping Chen and Dr. Kathryn Partin for their advice and critical evaluation during my graduate studies. I am blessed to have had the opportunity to work alongside such an accomplished scientist. I am also grateful to members of the laboratory with special thanks to Alisa Shaw, for teaching me nearly every technique used in my research today. As not to ramble I would simply like to thank Laurie Minamide, Dr. Barbara Bernstein and Dr. O'Neil Wiggan, whose comments and suggestions were very helpful to this thesis. I would also thank Ben Blackwell, for his work on preparing the medium from 7PA2 cells for isolation of A β , and Dr. Thomas B. Kuhn from University of Alaska, who suggested TNF α as a potential rod inducer.

TABLE OF CONTENTS

ABSTRACT.....	ii
ACKNOWLEDGMENTS	v
Introduction.....	1
Materials and Methods.....	14
Materials.....	14
Cell Cultures.....	14
Adenovirus Production.....	14
Adenoviral Infection.....	16
TNF α Preparation	16
Amyloid Beta Peptide Preparation.....	16
Alexa-CTxB Preparation.....	17
Fixation and Immunostaining.....	17
Live Cell Imaging.....	17
Analysis and Statistics.....	18
Results and Discussion	19
Creating MCP driven R21Q cofilin-RFP and NSE driven WT cofilin-RFP adenovirus	19
Quantification of cofilin-rod formation.....	23
The effect of photo stress in the induction of neuronal rods	26
TNF α induced cofilin-rod formation.....	29
A β d/t induced cofilin-rod formation	31
The fidelity of R21Q cofilin-RFP labeling rods induced by TNF α and A β d/t.....	33
The role of lipid rafts in TNF α - and A β d/t- induced rod formation	37
Future Directions for Research	45
References.....	47

Introduction

Actin, a major cytoskeletal protein in neurons, is involved in many different cellular processes that are essential for cell growth, differentiation, division, membrane organization and motility [Kuhn, et al., 2000]. Abnormalities in actin's assembly can result in aberrant structures.

Proteins of the actin-depolymerizing factor (ADF)/cofilin family are key regulators of actin dynamics. ADF/cofilin proteins enhance dynamics by increasing depolymerization from filament minus ends and also create more ends by severing filaments [Bamburg, et al., 1999]. Because cofilin's concentration in mammalian hippocampal neurons are 5-12 fold higher than ADF [Garvalov, et al., 2007], hereafter we will refer to these proteins only as cofilin.

Neuronal cofilin plays important roles in learning and memory pathways by modulating actin-rich dendritic spin architecture [Hotulainen et al., 2009]. Under cellular stress, cofilin forms complexes with actin that can alter cell functions [Bamburg, et al., 2002]. Recent findings suggest that hippocampal neurons exposed to neurodegenerative stimuli rapidly reorganize their actin cytoskeleton into rods, which are tapered cylindrical filamentous inclusions saturated with cofilin [Minamide, et al., 2000; Minamide, et al., 2010]. Overexpression or hyperactivation (excessive dephosphorylation) of cofilin under conditions of oxidative stress [Bernstein, et al., 2012] leads to formation of rods (Fig.1). Activation of cofilin, is stimulated by neurodegenerative stimuli including ATP-depletion [Minamide, et al., 2000] oxidative

stress [Minamide, et al., 2000; Kim, et al., 2008], excitotoxic glutamate [Minamide, et al., 2000], extracellular ATP [Homma, et al., 2008], and soluble forms of amyloid beta peptide [Maloney, et al., 2005, Davis, et al., 2009], each of which is a potential mediator of synaptic loss observed in both familial and sporadic AD [Ohm, 2007]. Familial AD is caused by a genetic mutations in pathways leading to enhanced amyloid beta production or reduced clearance, whereas sporadic AD, the most prevalent form, has many epigenetic causes and affects about 50% of all people reaching the age of 85 [Bamburg, et al., 2009].

Cofilin-actin rods, which form rapidly in response to stress, can grow to completely occlude the neurite in which they form causing microtubule loss [Minamide, et al., 2000] and thus inhibit vesicular transport [Jang, et al., 2005; Cichon et al., 2012]. Neuronal cytoplasmic rods accumulate within neurites where they disrupt synaptic function and are a likely cause of synaptic loss without neuronal loss, as occurs early in dementias [Bamburg, et al., 2010], which can explain virtually all aspects of AD progression.

Different rod-inducing stimuli target distinct neuronal populations within the hippocampus [Davis et al., 2009; Bamburg, et al., 2010]. Stress-induced formation of rods in neurons as an initiator for several neurodegenerative diseases is intriguing. As an early event in the neurodegenerative cascade, rod formation is an ideal target for therapeutic intervention that might be useful in treatment of many different neurological diseases [Bamburg, et al., 2010].

When fluorescently tagged wild type cofilin is used to image the formation of rods in living cells, its overexpression alone induces an increase in rods (Fig.2), which is exacerbated by the photo-stress of microscopy [Bernstein, et al., 2006; Cichon, et al., 2012]. Both imaging-induced and overexpression-induced rod formation confound the interpretation of studies that are looking for rod formation in response to a particular unique stimulus. Thus one aim of this thesis is to determine if lowering the expression of WT cofilin-RFP by using promoters that reduce the steady-state levels of expression would be sufficient to decrease spontaneous rod formation. To address this aim, we compared the cytomegalovirus (CMV) promoter, which maintains a high level of expression (strong promoter), with the mouse cofilin promoter (MCP) and the neuronal specific enolase (NSE) promoter, each of which maintains a lower level of expression. The expression level driven by these three promoters was quantified in Fig 3 from western blot.

A second aim of this thesis is to characterize a mutant cofilin that will not induce rods when overexpressed or when expressed in cells that are photostressed but which will get incorporated into rods formed from endogenous proteins and thus serve as a live cell imaging tag for rod formation in response to specific rod-inducing stimuli. To address this aim, site directed mutagenesis was performed by others on cofilin surface residues to identify mutations which are inhibited in rod incorporation when overexpressed, but which will be incorporated into rods formed by endogenous cofilin. One such mutant, R21Q was identified (Fig.4). It has about a 10 fold weaker interaction with F-actin than cofilin wild type [Alisa Shaw, unpublished data], yet it

can still be incorporated into induced rods (Fig.5). Previous studies characterized the ability of R21Q cofilin- RFP driven by a CMV promoter to label rods induced by ATP-depletion [Chi W. Pak, Ph.D. Thesis]. Here we further characterized its fidelity in labeling rods induced by other stress agents and when its expression is driven by other promoters.

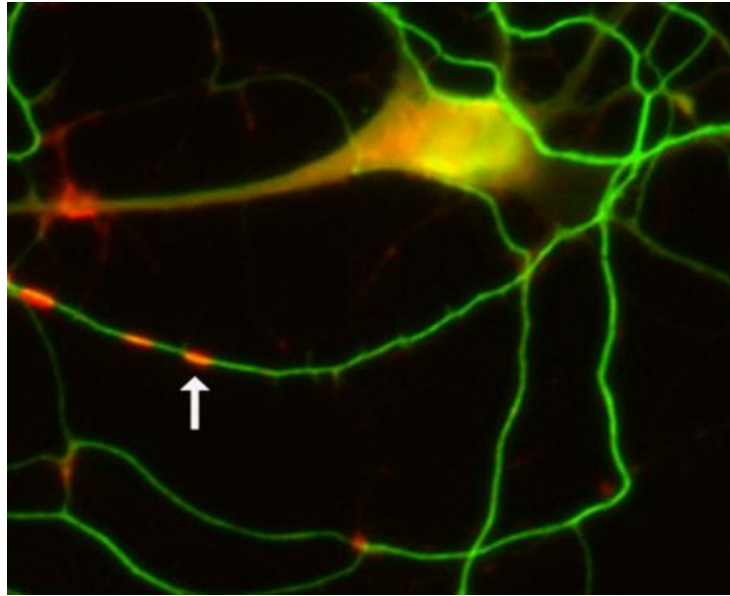


Figure 1. Immunostained cofilin rods in cultured neurons.

Dissociated E18 rat hippocampal neurons were cultured for 5 d *in vitro* (div), ATP-depleted for 30 min, and then returned to normal medium for 24 h. Cells were fixed and double immunostained for cofilin (Texas Red) and phosphorylated neurofilament high-molecular-mass subunit (NFH; fluorescein). Cofilin-containing rods were observed in both axons and dendrites. Shown here are rods (red) formed in neurofilament-H (NFH) positive axons (green).

[Minamide, et al., 2000]

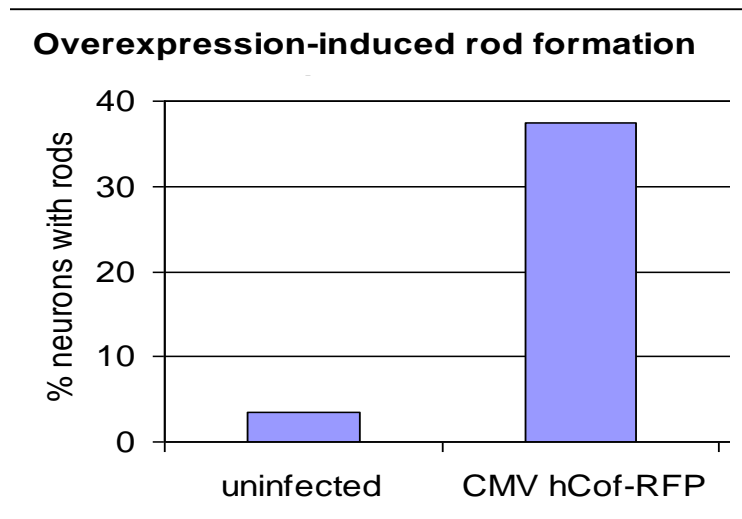


Figure 2. Overexpression of wild type cofilin induces rod formation.

E18 Hippocampal neurons were either uninfected or infected at 3 div with an adenovirus for expressing CMV-driven WT cofilin-RFP. Two days after infection, with no additional stress, cells were fixed and stained for cofilin and the percent of neurons containing rods was scored. Overexpression of WT cofilin-RFP promoted higher level of rod formation in neurons even in the absence of other stimuli.

[Alisa Shaw, unpublished data]

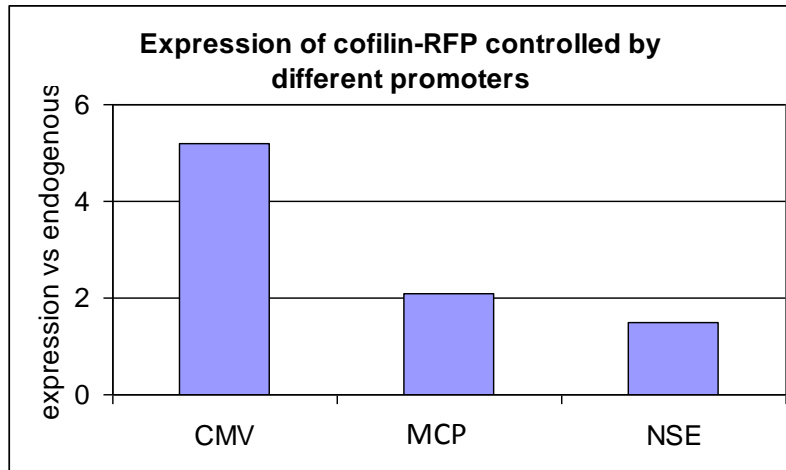


Figure 3. Expression of cofilin-RFP controlled by different promoters.

N2A mouse neuroblastoma cells were infected with adenoviruses in which expression of cofilin-RFP was controlled by CMV, MCP, or NSE promoters. The amount of expressed cofilin-RFP versus endogenous cofilin was quantified from western blot after 72 h. The expression of cofilin-RFP driven by CMV promoter was about 5 fold higher than the endogenous protein, 2 fold of MCP, and about 1 of NSE.

[Alisa Shaw, unpublished data]

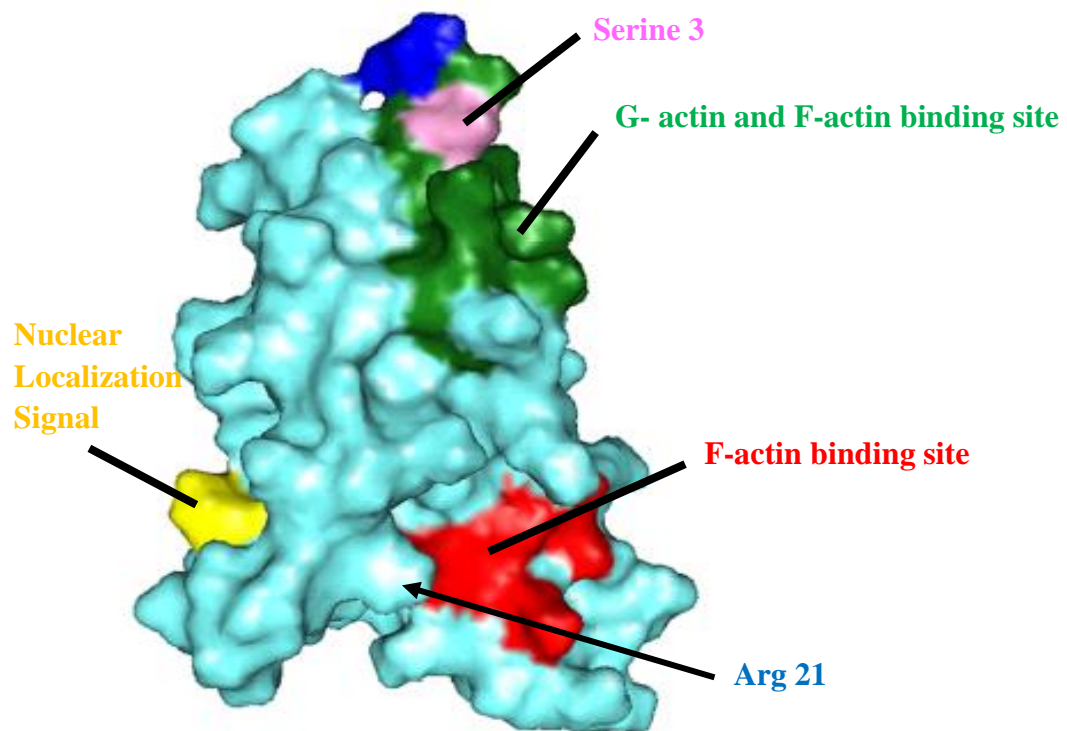


Figure 4. Model of cofilin with R21 site shown.

The R21Q mutant was identified in a screen for cofilin mutants that did not form cofilin-actin rods when overexpressed in HeLa cells. The residue, R21, is surfaced-exposed, but outside the characterized F- and G-actin binding surfaces. The 3-D structure of cofilin was generated in PyMol using NMR data of human cofilin.

[Chi W. Pak, Ph.D. Thesis]

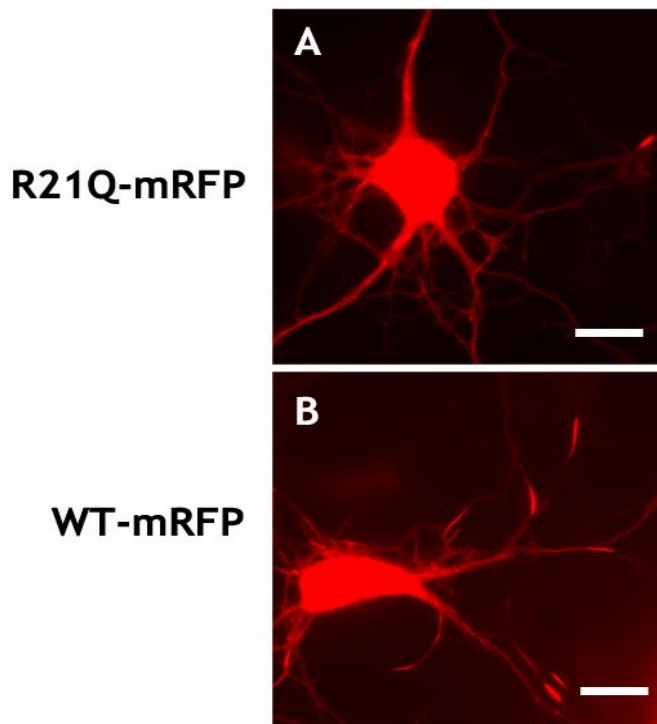


Figure 5. The R21Q cofilin-RFP incorporates into endogenous cofilin-actin rods but forms less spontaneous rods than WT cofilin-mRFP.

WT and R21Q cofilin are C-terminal chimeras with monomeric RFP (mRFP). (A, B.) Both R21Q and WT cofilin-RFP incorporate into spontaneous rods. However, rods generated by overexpressing WT cofilin-RFP are more numerous, in a higher percentage of the neurons, and are larger in size. Bar=15 μ m

[Chi W. Pak, Ph.D. Thesis]

Cofilin-actin rods induced by physiologically relevant [McDonald JM. et al., 2010, Davis, et al., 2011] A β d/t and TNF α require the cellular prion protein (PrP^c), a GPI-linked protein that is a component of membrane lipid rafts. PrP^c can signal to activate NADPH oxidase (NOX) to generate reactive oxygen species (ROS). Lipid rafts are cholesterol/sphingolipid- enriched detergent-resistant membrane domains in which many membrane receptors associate. Normally lipid rafts are very small domains, involved in transmembrane signaling. Cofilin may be concentrated underneath raft domains because it binds to phosphatidylinositol-bis-phosphate (PIP₂) [Zhao H, et al., 2010], which is enriched in the cytoplasmic membrane leaflet of rafts, the site where NOX generates the reactive oxygen.

When cells are treated with TNF α or A β d/t, the lipid raft may coalesce into fairly large domains on the membrane surface. Based on one experiment in which rods were induced by A β d/t and lipid rafts were labeled with an Alexa-labeled cholera toxin subunit B (CTxB), rod staining was found underneath regions where lipid raft coalescence occurred (Fig.6). We don't know how frequently this occurs, whether the lipid rafts form first and signal the formation of rods, or whether the rods form and enhance lipid raft coalescence.

Our hypothesis is that TNF α or A β d/t [Lauren, et al., 2009] bind directly or indirectly to the cellular prion protein PrP^c enhancing the coalescence of lipid raft domains to activate NOX and generate bursts of ROS, producing reactive oxygen, which can cause the cofilin inter-molecular disulfide bond to form, leading to formation of rods in sensitive neurons [Bernstein, et al., 2012] (Fig.7).

The final aim to be addressed in this thesis is to determine if coalescence of lipid rafts into larger macro-domains a prerequisite for A β - and TNF α -induced rod formation. Our hypothesis is that raft coalescence precedes rod formation. We will follow lipid raft coalescence and rod formation simultaneously, adding Alexa 488-CTxB to the medium to label G_M1 gangliosides and infecting neurons with adenovirus expressing R21Q cofilin-mRFP to follow rod formation. Finding raft coalescence after rod formation would suggest that rods are able to organize membrane lipids.

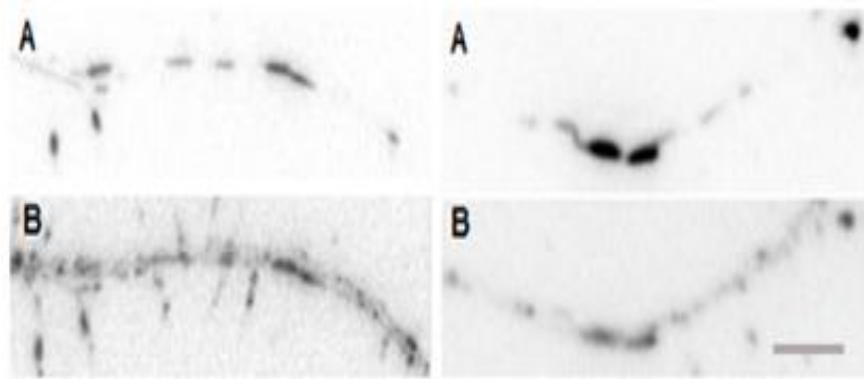


Figure 6. Rods form in regions of neurites where raft domains have coalesced. (A) panels show inverted fluorescence of cofilin-stained rods induced by TNF α . Lower (B) panels show corresponding lipid rafts stained with Alexa-CTxB. The major regions of raft coalescence correspond to rod staining regions. Bar=10 μ m. [J. R. Bamberg, unpublished data]

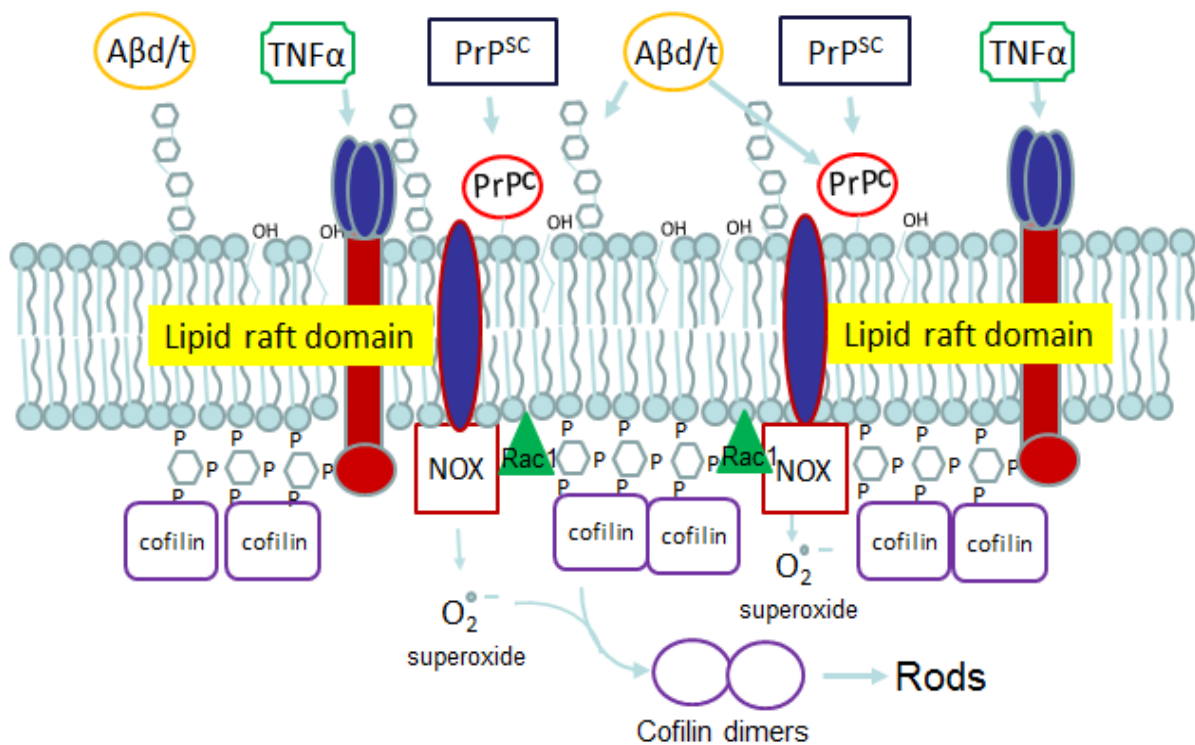


Figure 7. Model of lipid raft domain showing PrPc-mediated ROS production and rod formation in response to Aβd/t and TNFα.

TNFα or Aβd/t binds to their receptors. In the case of Aβd/t this is PrP^C which may also be the receptor for TNFα. Unknown mechanisms mediate the signaling to NADPH oxidase. Lipid rafts are enriched in PIP₂, a cofilin-binding lipid putting the cofilin at the site for ROS generation. Formation of cofilin inter-molecular disulfide bond can lead to formation of rods in sensitive neurons.

[J. R. Bamberg, unpublished schematic]

Materials and Methods

Materials.

All chemicals were reagent grade and were obtained from Sigma. All culture reagents were from Life Technologies (Invitrogen).

Cell Cultures.

HEK 293 cells were grown in tissue culture dishes in high glucose Dubelco's Modified Eagle Medium (HGDMEM) containing 10% FBS (Hyclone Laboratories).

Frozen cell stocks of Sprague-Dawley E18 rat hippocampal neuronal cultures were prepared from E18 brain dissection according to the method of Bartlett and Banker [1984]. Dissociated neurons were plated on poly-D-lysine coated no.1 German glass coverslips (22 x 22 mm; Carolina biological Supply Co.) fixed to the bottom of drilled out T25 tissue cultural flask with aquarium sealant. Sealant was cured for 24 hours before cells were plated to minimize leeching of acid into the growth medium. Cells were grown in neurobasal medium with B27 supplement (100ul/10ml) and glutamax (25ul/10ml) at a density of 2×10^4 cells/120 mm² [Brewer et al.1993].

Adenovirus Production.

Adenoviruses were made using the AdEasy system described by Minamide et al. [Minamide, et al. 2003].

Cloning was performed to create the mouse cofilin promoter (MCP) driven R21Q cofilin-RFP and neuronal specific enolase (NSE) promoter driven WT cofilin-RFP in adenovirus. (The MCP-driven WT cofilin-RFP, NSE driven R21Q cofilin-RFP, and cytomegalovirus (CMV) promoter driven WT/R21Q cofilin-RFP had been made in the lab previously by Alisa Shaw).

The cDNA for R21Q cofilin-RFP was excised from the CMV R21Q cofilin-RFP plasmid vector by using restriction enzymes Not I & Xba I. The cDNA fragment was then ligated into pShuttle MCP. After determining that the insertion was correct by Not I & Xba I digestion and gel analysis, the vector was linearized with the restriction enzyme Pme I and electroporated into BJ5183/AdEasy 1 electrocompetent E coli cells, allowing the bacteria to carry out homologous recombination between the pShuttle and AdEasy1. After plating the electroporation mixture on plates of LB-Kan medium, colonies were picked and inoculated into 10 mL of LB-Kan and grown overnight. Following a subsequent miniprep, another test digest was conducted with Pac I to assess the recombination. Frozen glycerol stocks of clones with the correct insert were then created. The recombined DNA was linearized by Pac I and transfected into Human Embryonic Kidney (HEK) 293 cells, which provides in trans the essential E1a gene product missing from the virus which is required for virus replication and packaging.

High titer virus was obtained by successive rounds of infection in 293 cells. The infected 293 cells were harvested, and the infectious but replication-incompetent virus was released from the cells through freeze-thaw cycles (He et al, 1998). Finally, MCP

driven R21Q cofilin-RFP in adenovirus was harvested. The NSE driven WT cofilin-RFP in adenovirus was made similarly. The viruses were titered according to the method described by Minamide et al. [2003].

Adenoviral Infection.

Cultures were maintained in a 5% CO₂ incubator at 37 °C for 3 days before infection at 100-300 multiplicity-of-infection (m.o.i.). Infected cells were incubated overnight before half of medium was replaced. Experiments were performed 4 days post infection.

TNF α Preparation.

Tumor necrosis factor α was purchased from Enzo life sciences. It was dissolved in neurobasal medium with 1% BSA at 50 μ g/mL and used in neuronal culture at a final concentration of 50 ng/mL (2.87 nM) [concentration selected based upon dose-response by Walsh and Minamide, 2011, unpublished data]. Cells with a medium change served as controls. After 20 hours treatment, cells were imaged or stained with Alexa-CTxB and then fixed.

Amyloid Beta Peptide Preparation.

A β d/t was prepared from the culture medium of 7PA2 Chinese hamster ovary cells expression a human amyloid precursor protein with AD mutations. Unless noted otherwise it was used at 1X concentration, the concentration released into the medium, estimated at 250 pm [Davis, et al., 2011]. Cells with a medium change served as

controls. After 24 hours treatment, cells were imaged or stained with CTxB and then fixed.

Alexa-CTxB Preparation.

For staining of surface G_{M1} ganglioside, neurons were incubated with Alexa Fluoro 488 labeled CTxB at 50 ng/mL for 15 min at 37 °C. Then, cells were imaged or directly fixed.

Fixation and Immunostaining.

Neurons were fixed for 20 min, at room temperature in 4% formaldehyde in PBS. Neurons were methanol (-20 °C) permeabilized for 3 min and blocked in 2% goat serum/1% bovine serum albumin in TBS before immunostaining. Primary antibodies: affinity purified rabbit 1439 IgG to chick ADF (75 ng/μL), which cross-reacts with mammalian ADF and cofilin, was added to the cells for 2 hours at room temperature. The cells were rinsed 5X with TBS (10 mM Tris pH 8.0, 150 mM NaCl). Secondary antibody was Alexa 647 goat anti-rabbit, used at 1:400 dilution, and added to the cells for 1 hour at room temperature. After washing, neurons were treated with ProLong Gold Antifade and covered with a round coverslip that fit in the glass-bottom dish.

Live Cell Imaging.

Fluorescence microscopy was used to observe rod formation in live hippocampal neurons. Images were acquired on an Olympus spinning disk confocal microscope using a 60X oil objective, 300 ms exposure times, single fields exposed at each time.

Series of time-lapse images were captured every 30 seconds, using the confocal microscope with a heated 37 °C, 5% CO₂ controlled stage for a total of 2 hours. All captured images were inverted to enhance the appearance of rods for subsequent analysis and presentation.

Analysis and Statistics.

For quantification of cells containing rod structures, neurons with rods were counted from randomly selected fields on each coverslip, and cells containing rod structures were then expressed as a percentage of the total number of cell. To ascertain the regional distribution of rods, the mean number of rods per field from at least 20 random fields was recorded. All experiments were repeated in triplicate using independently prepared cell cultures. Levels of significance were calculated using the student “T-test” and are reported as $p < 0.05$ or $p < 0.005$ as appropriate.

Results and Discussion

Creating MCP driven R21Q cofilin-RFP and NSE driven WT cofilin-RFP adenovirus

To develop a probe for following rod formation in vivo we wanted to make vectors for achieving low levels of expression of WT cofilin-RFP as well as for expressing different levels of the R21Q cofilin-RFP. Three promoters were selected for achieving different expression level: the strong cytomegalovirus (CMV) promoter, the moderate mouse cofilin promoter (MCP), and the weaker neuronal specific enolase (NSE) promoter. Promoter strength is inferred from the steady state level of cofilin-RFP expression measured by western blotting. Adenoviruses containing MCP driven WT cofilin-RFP, NSE driven R21Q cofilin-RFP, and CMV driven WT/R21Q cofilin-RFP had been made in the lab previously. New adenoviruses were made to express R21Q cofilin-RFP behind MCP and WT cofilin-RFP behind the NSE promoter to give the complete set.

Cloning was performed to create adenoviruses for the MCP driven R21Q cofilin-RFP as outlined in Fig.8 and NSE promoter driven WT cofilin-RFP as outlined in Fig.9. Briefly, the cDNA encoding mRFP-tagged R21Q cofilin was cloned into pShuttle MCP using standard molecular-cloning techniques. Recombination of the cDNA into the adenoviral genome was accomplished by electroporating into a recombinase-positive BJ5183 E coli. strain carrying a modified adenoviral genome (AdEasy). To produce functional adenovirus, the AdEasy-cDNA construct was

linearized and transfected into HEK293 cells, which provide an essential viral replication gene in trans. After several amplifications in HEK293 cells, a high titer of adenovirus was harvested by iterative freeze-thawing and aliquots were stored at -80 °C until their use. The NSE driven WT cofilin-RFP in adenovirus was made similarly.

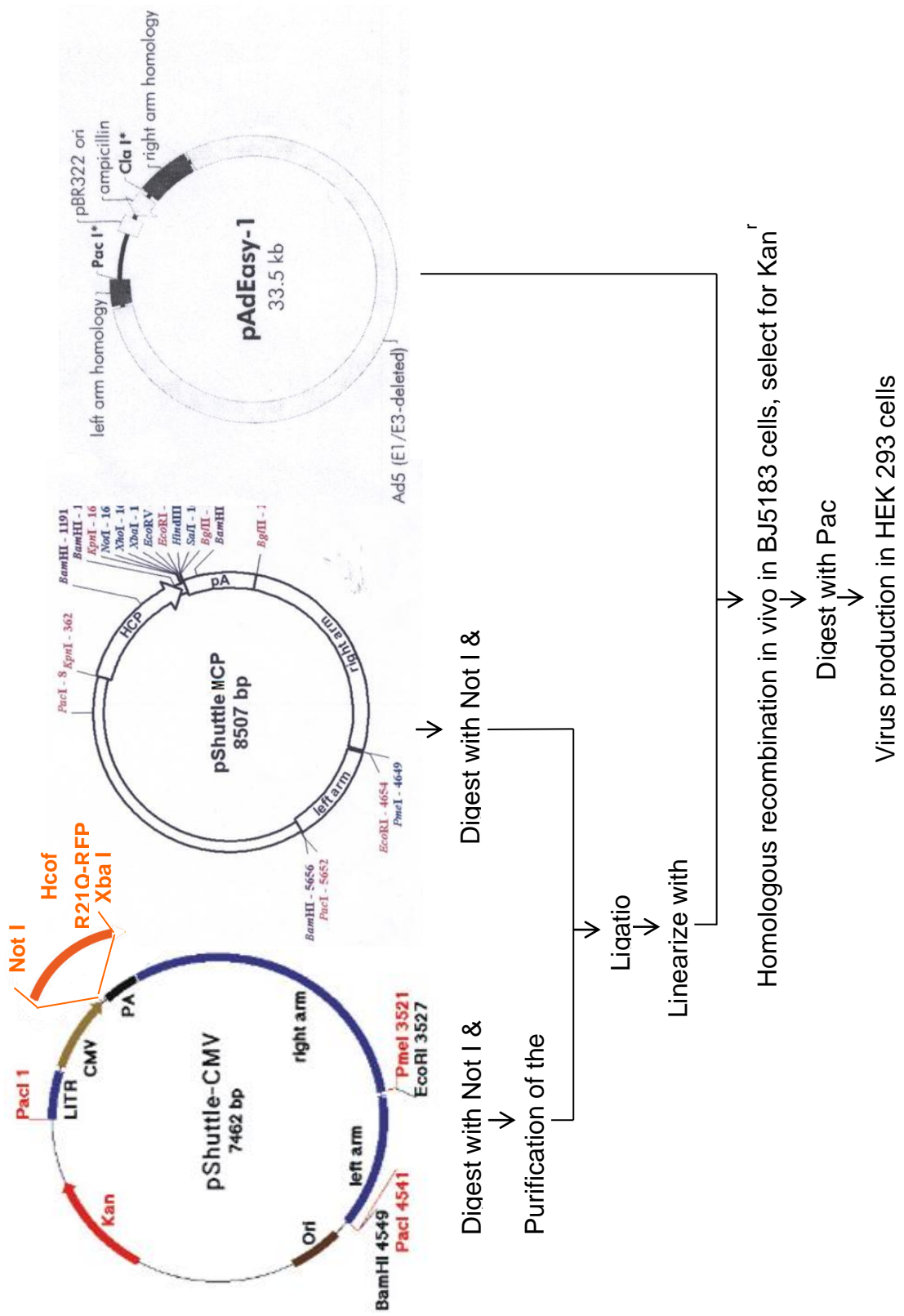


Figure 8. Flow diagram of generation of MCP driven R21Q cofilin-RFP in adenovirus.

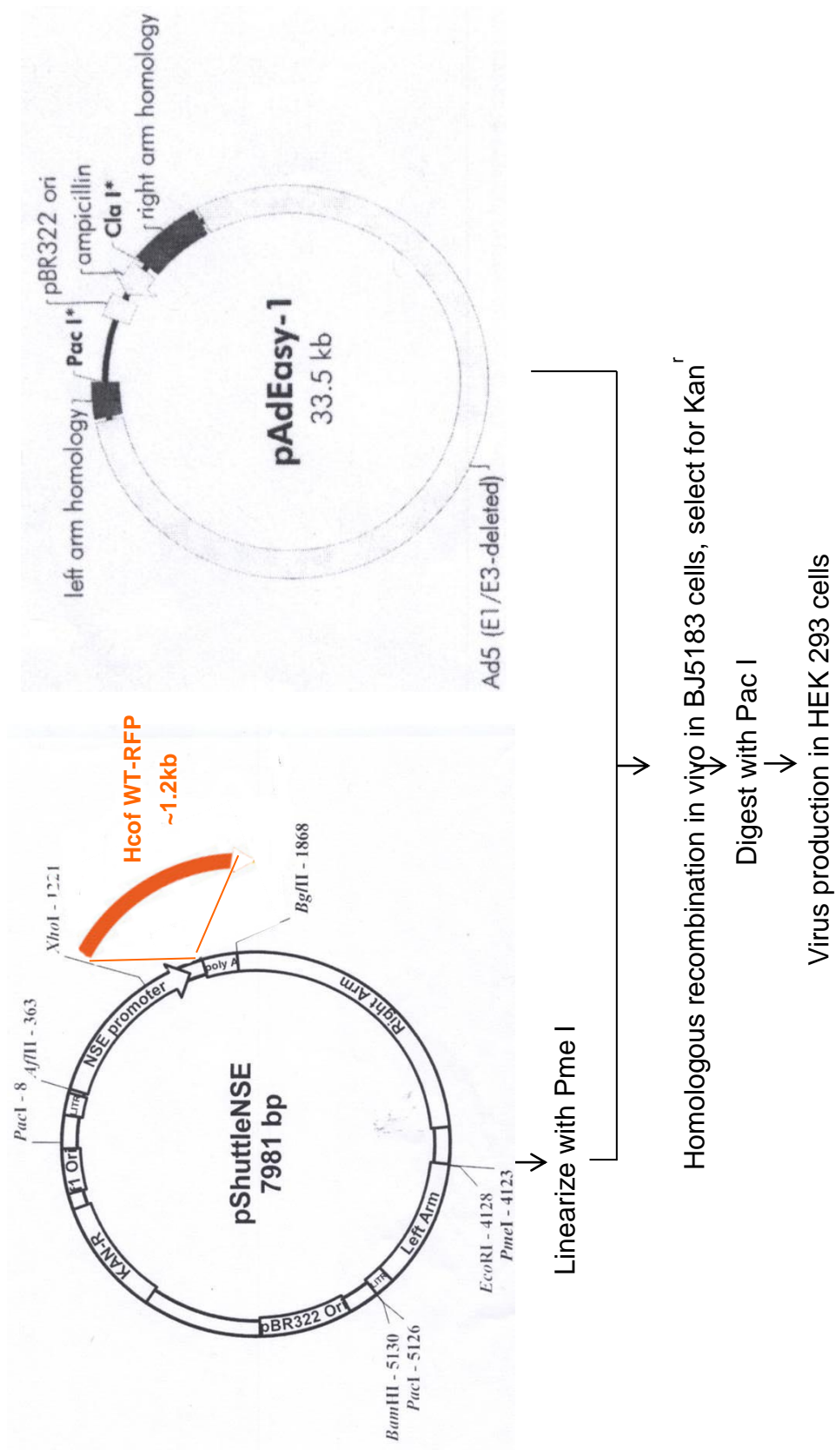


Figure 9. Flow diagram of generation of NSE driven WT cofilin-RFP in adenovirus.

Quantification of cofilin-rod formation

Because cofilin-actin rods occur at low frequency in untreated cultures, the presence of rods alone could not be used to assess rod induction from the expression of various cofilin constructs. It is also important to assess the stress induced by adenoviral infection by using a control adenovirus from which RFP, but no cofilin, is expressed behind a CMV promoter. Two indices of rod formation were quantified: percent-rod index and number-rod index. Percent-rod index is defined as the percentage of neurons that form at least one cofilin-actin rod. For each experiment, at least 100 neurons were included in this analysis. Number-rod index is defined as the average number of rods counted in each field selected at random. For each experiment, at least 20 non-overlapping fields were included in the analysis.

Hippocampal neurons, cultured in glass bottom dishes for 3 days, were infected with WT or R21Q cofilin-RFP, driven by CMV, MCP and NSE or by the virus expressing only RFP (CMV-RFP). Two days post infection, neurons were fixed and the control group (infected with CMV-RFP) was also immunostained for cofilin (Alexa 488) and the percent-rod index and number-rod index were scored.

Percent-rod index for WT cofilin was greatest for the high expressing CMV promoter, slightly lower for the moderate MC promoter and lowest for the weaker NSE promoter (Fig. 10). However, even for the weakest promoter, the percent rod index and number rod index are significantly higher than for the controls, demonstrating that even low expression of WT cofilin increases the formation of spontaneous rods. Significantly, both the percent rod index and number rod index was

at control levels for all neurons expressing R21Q cofilin-RFP regardless of the promoter used to drive expression (Fig. 10). The percent-rod index indicates how many neurons are responding, however, it does not indicate how vigorously the neurons responded. From the number-rod index, cells expressing WT cofilin-RFP infected driven by the CMV promoter had the highest (7 fold over control) number of rods in the counted field (Fig.10b), with MCP and NSE promoters driving enough cofilin expression to give about a 2 fold increase in rod numbers over controls.

Although driving lower expression of the WT cofilin-RFP with the MC and NSE promoters resulted in fewer spontaneous rods than when the CMV promoter was used, the numbers are still well above the controls in all cases demonstrating that expression of WT cofilin-RFP will not be useful for monitoring induced rods. The R21Q cofilin-RFP will incorporate into rods formed from endogenous protein (at the control level), but its expression even to very high levels, such as those induced by the CMV promoter, does not enhance spontaneous rod formation.

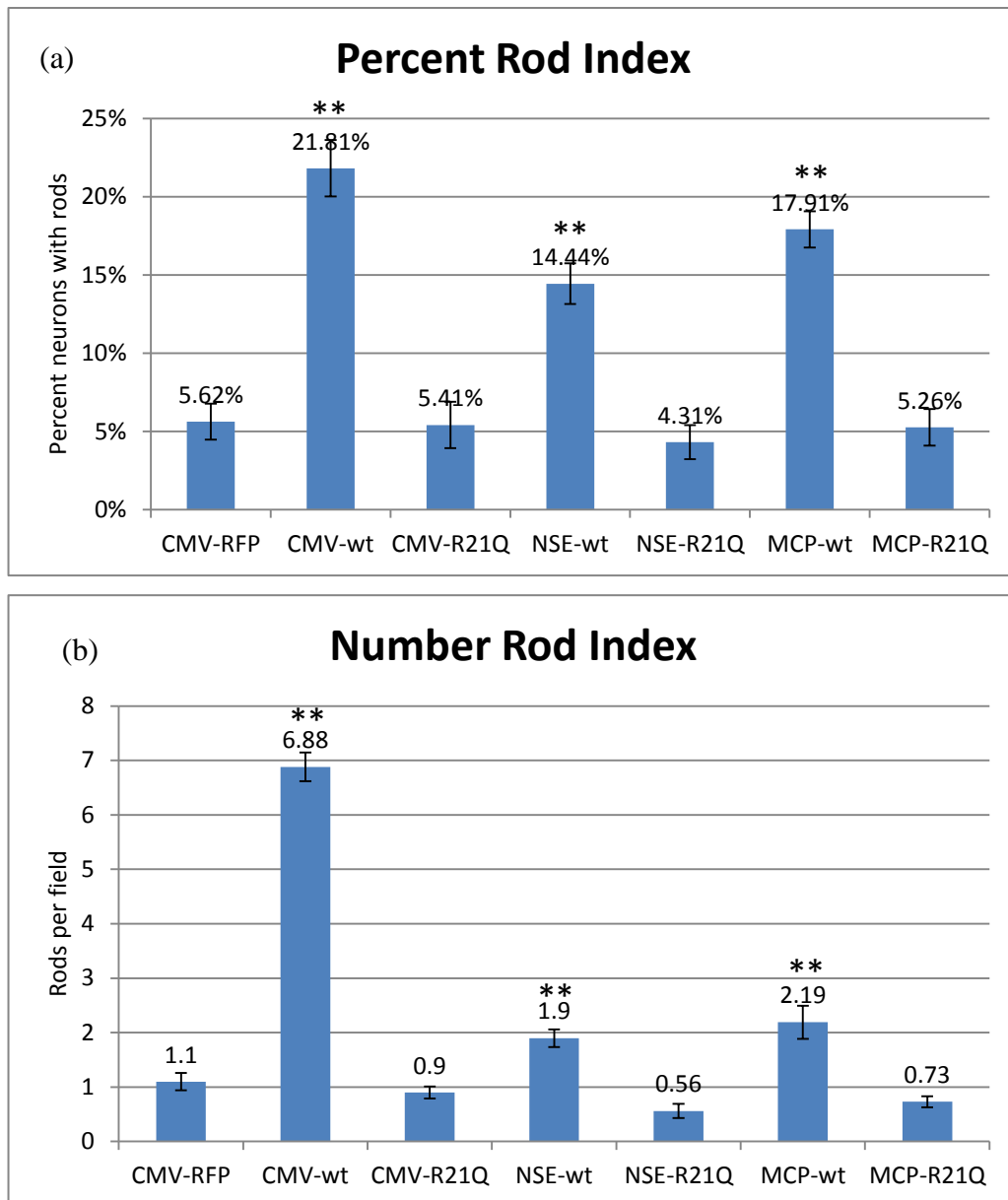


Figure 10. Quantification of rod formation in hippocampal neurons expressing either WT or R21Q cofilin-RFP.

(a) The fraction of neurons that formed spontaneous rods is at control levels for R21Q cofilin-RFP overexpression regardless of promoter, whereas all WT cofilin-RFP expressing neurons were significantly above controls.

(b) The total rod response for neurons expressing R21Q cofilin-RFP are at or below the control level regardless of the promoter driving expression whereas WT cofilin-RFP expressing neurons are all significantly above the control by 2 to 7 fold.

(**Significant at $p < 0.005$, compared to the CMV-RFP control group)

The effect of photo stress in the induction of neuronal rods

Imaging of cells expressing fluorescently-tagged chimeras of cofilin can enhance rod formation above that caused by overexpression alone [Bernstein et al., 2006], which confounds the interpretation of microscopy studies of rod formation induced by a particular unique stimulus (such as A β). To test the effect of photo stress in the induction of neuronal rods, E18 hippocampus neurons were infected with adenovirus for CMV/ NSE/ MCP driven cofilin wild type and R21Q cofilin-RFP. Photo stress was measured 4 days post infection. Time-lapse imaging was performed in two hour session in which a total of 240 images were acquired at 30 second intervals between images.

After the two hour photo stress, there was obvious rod formation in the neurons expressing wild type cofilin-RFP. The expression driven by MC and NSE promoters result in fewer photo stress-induced rods than when expression is driven by the CMV promoter (Fig.11). In the R21Q cofilin-RFP expressing cells, we did not observe newly formed rods (Fig.11e), regardless of promoter. We conclude that the R21Q cofilin-RFP mutant can be used as a live cell imaging tag for rod formation in response to specific rod-inducing stimuli. We will now apply R21Q cofilin-RFP to study rod formation in live cells.

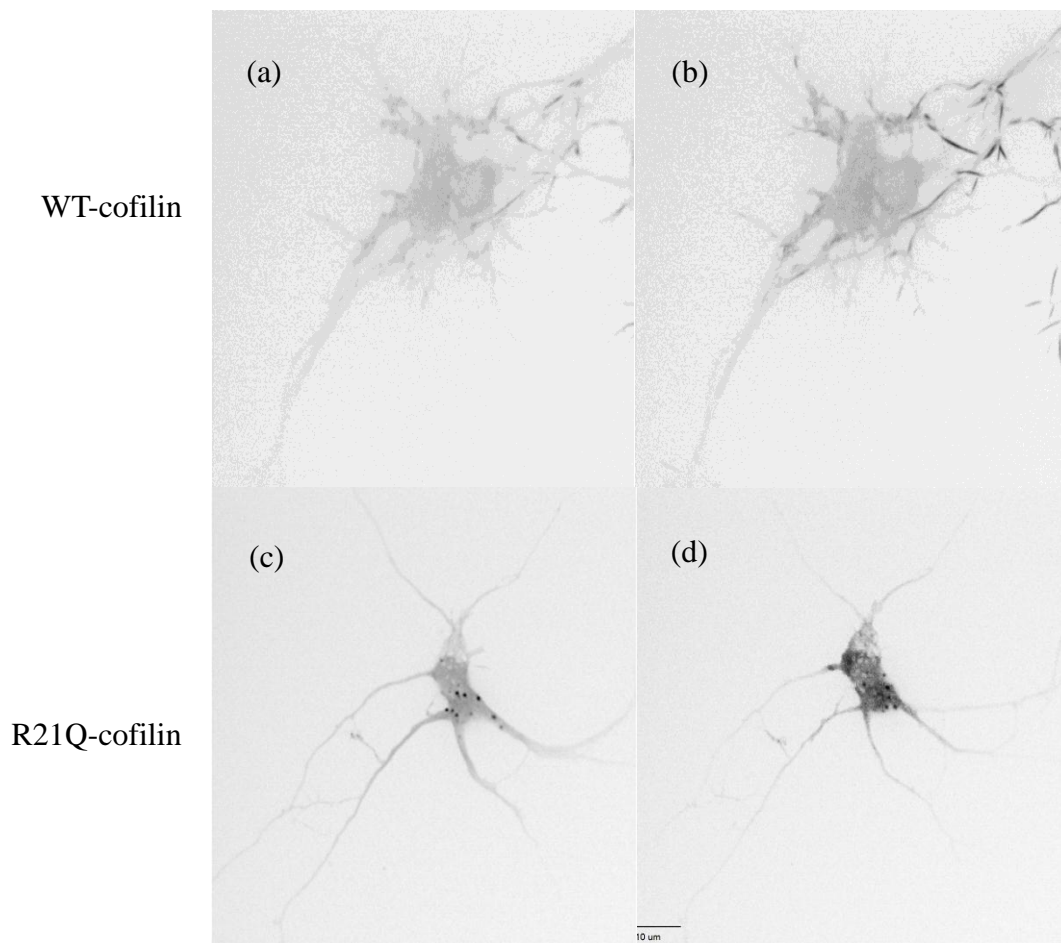


Figure 11. Photo stress induces rod formation.

E18 Hippocampal neurons were infected 3 div with adenovirus for expressing CMV-driven WT cofilin-RFP (a,b) or R21Q cofilin-RFP (c,d). Two days after infection, cells were imaged in a two hour session at 30s intervals using the confocal microscope. (a) (c) were before starting the photo-stress. (b) (d) were the after the photo stress. Note the abundance of new rods in (b).

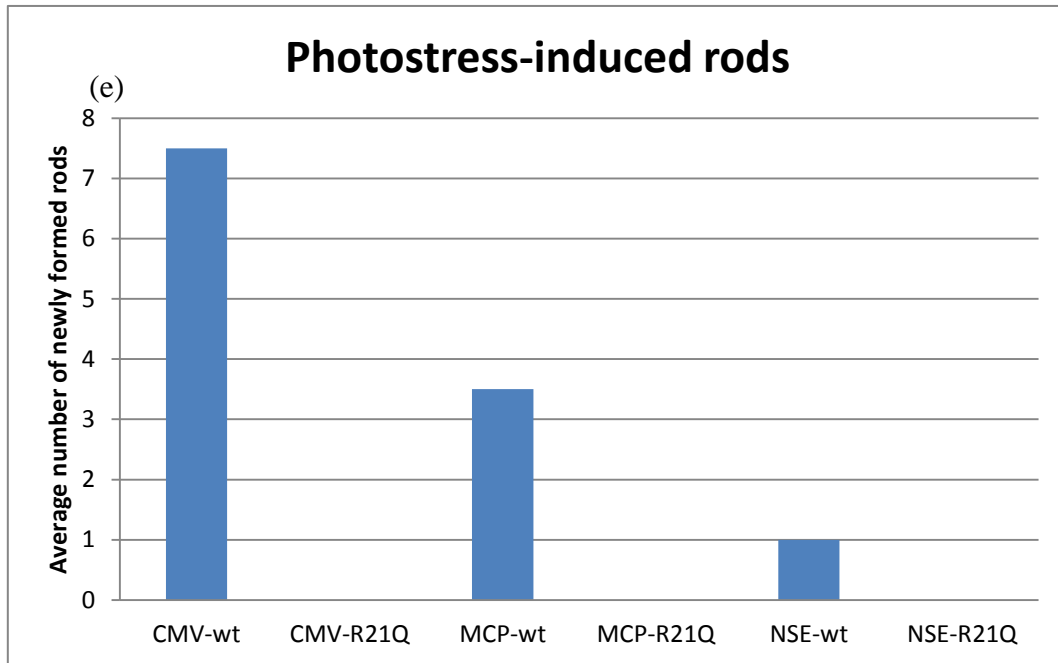


Figure 11. (e) The quantification of the average number of rods induced by photo-stress in each neuron. The hippocampal neurons were infected by adenoviruses expressing WT cofilin-RFP or R21Q cofilin-RFP, driven by CMV, MCP and NSE. Three days post infection, cells were photo-stressed in a 2 hour session, at a 30 second interval. Neurons expressing WT cofilin-RFP generated a lot of spontaneous rods over the 2 hour session. No rods were observed after the photo stress in any of the R21Q cofilin-RFP expressing neurons, regardless of the promoter driving expression.

TNF α induced cofilin-rod formation

Since expression of R21Q cofilin-RFP does not increase rods even when it is overexpressed behind a strong promoter or during photo-stress, we used it to examine rod formation in neurons treated with TNF α . TNF α is a cytokine involved in systemic inflammation. The concentration of TNF α used in rod induction and the time for treatment were determined by a dose-response and time course experiment, from which the TNF α at 50 ng/mL (2.87 nM) induces near maximal rod response by 24h.

Hippocampal neurons, cultured in glass bottom dishes for 3 days, were infected with R21Q cofilin-RFP, driven by CMV, MCP or NSE promoters. The control group was infected with virus CMV-RFP to express RFP alone. Two days post infection, neurons were left untreated or treated with TNF α . Neurons were fixed after 24 hours and the percent-rod index and number-rod index were scored.

The fraction of neurons that formed rods in response to TNF α is about three fold higher than the fraction of untreated neurons with spontaneous rods (Fig.12a), although there is no significant difference between the different promoters. The percent-rod index is virtually identical between the neurons infected with control virus (RFP only) and any of the different R21Q cofilin-RFP viruses, regardless of promoter. From the number-rod index, neurons infected with any of the different R21Q-cofilin-RFP viruses and treated with TNF α give a 2-3 fold measure in rod numbers over the controls (Fig.12b). And both the percent rod index and number rod index was at control levels for all neurons expressing R21Q cofilin-RFP regardless of promoter.

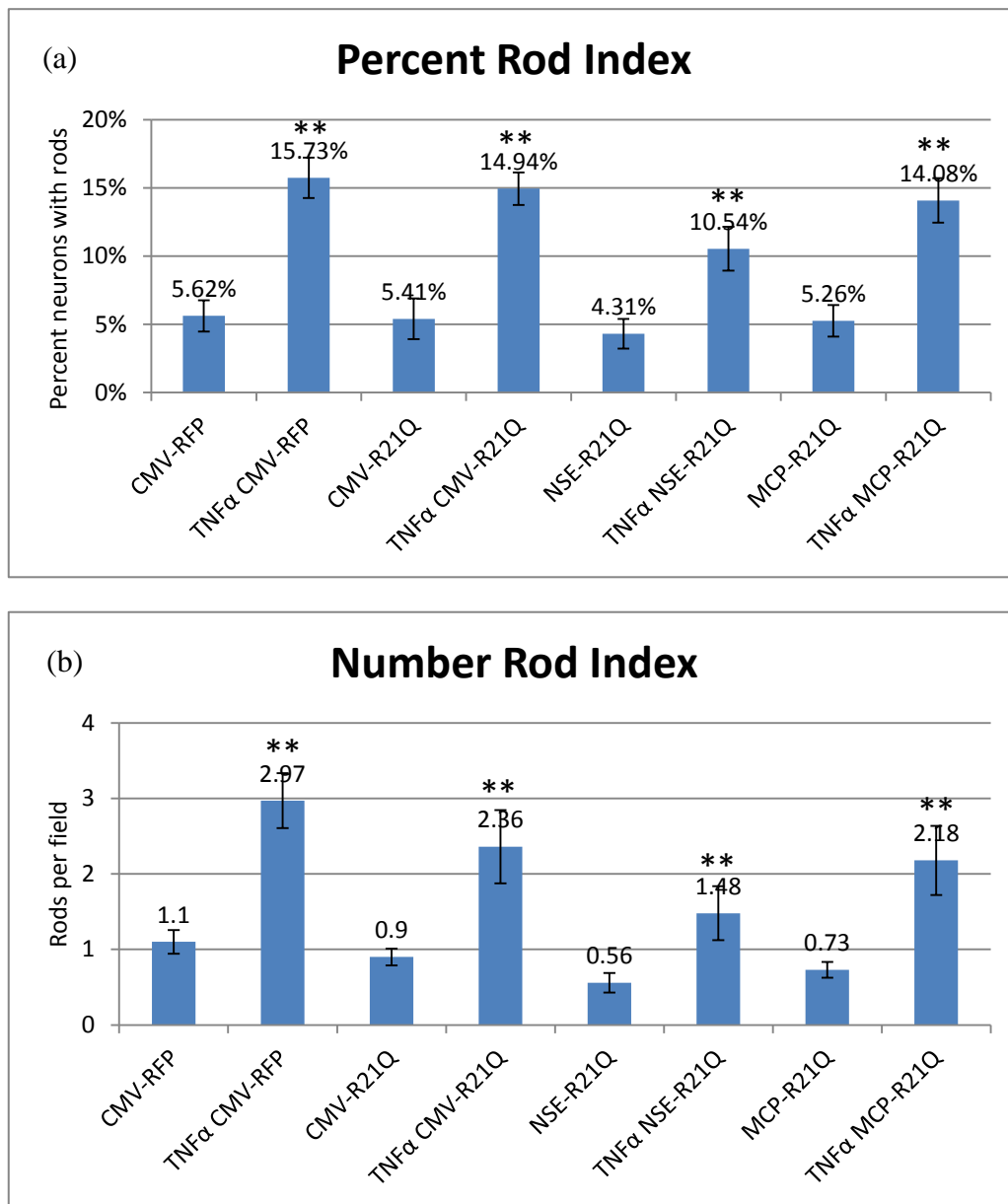


Figure 12. Quantification of rod formation in response to TNF α treatment.

(a) The fraction of neurons that formed rods after treatment with TNF α is 2.5 to 3 fold higher than for the untreated neurons.

(b) The number of rods per field in TNF α treated neurons expressing R21Q cofilin RFP is 2.5-3 fold higher than the controls regardless of promoter driving expression.

None of the R21Q cofilin-RFP expressing cultures that were untreated with TNF α had rod numbers of percent neurons with rods that different from controls.

(**Significant at $p < 0.005$, compared to the CMV-RFP control group)

A β d/t induced cofilin-rod formation

We then examined rod formation in neurons treated with A β d/t at 1X concentration (~250 pM) for 24 h. Similar to the result of treatment with TNF α , the fraction of neurons that formed rods in response to A β d/t is 2-3 fold higher than the fraction of untreated neurons with spontaneous rods (Fig.13a), with no significant difference between the different promoters. The percent-rod index is virtually identical between the neurons infected with control virus (RFP only) and all of the different R21Q cofilin-RFP viruses, regardless of promoter. From the number-rod index, neurons treated with A β d/t regardless of the promoter driving expression give a 2 fold increase over the controls (Fig.13b).

Both the percent rod index and number rod index for treatment with A β d/t are similar to the result of TNF α induced rod formation. Rod formation in response to TNF α or A β d/t is significantly above the untreated controls, regardless of promoter.

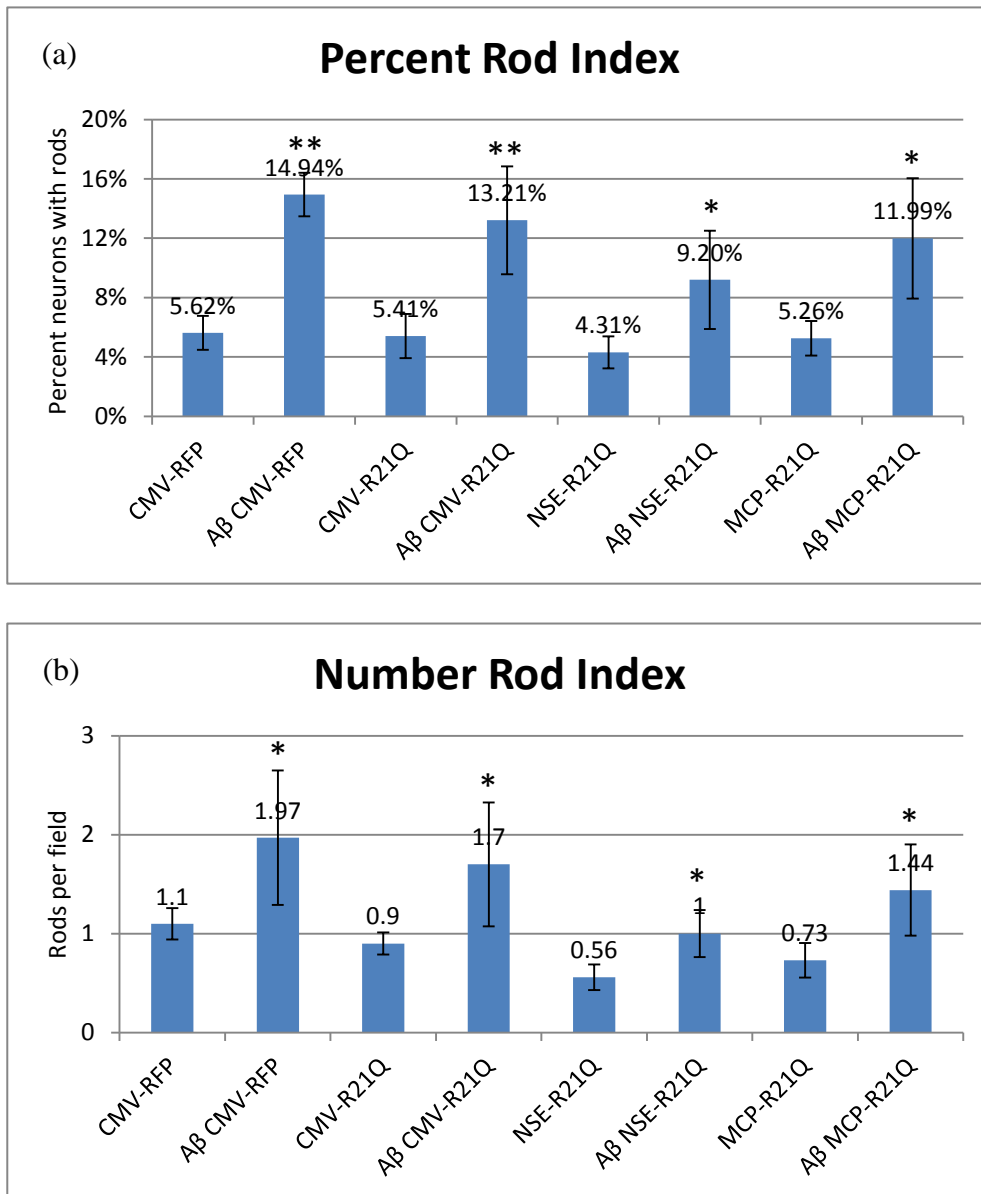


Figure 13. Quantification of rod formation in response to Aβd/t treatment.

(a) The fraction of neurons that formed rods after treatment with Aβd/t is 2.5 to 3 fold higher than for the untreated neurons.

(b) The number of rods per field in Aβd/t treated neurons expressing R21Q cofilin RFP is 2 fold higher than the controls regardless of promoter driving expression.

(*Significant at $p < 0.05$, **Significant at $p < 0.005$, compared to their appropriate non-Aβd/t-treated control group)

The fidelity of R21Q cofilin-RFP labeling rods induced by TNF α and A β d/t

To be useful as a quantitative live-cell reporter for rod formation, the R21Q cofilin-RFP must incorporate into all cofilin-actin rods formed from endogenous proteins. The R21Q cofilin-RFP rods completely co-localized with rods detected by immunostaining for cofilin in the ATP depleted treated neurons (Fig.14) [Chi W. Pak, Ph.D. Thesis].

To determine R21Q cofilin-RFP's fidelity for detecting rods in response to TNF α and A β d/t treatment, rat hippocampal neurons expressing R21Q cofilin-RFP, were treated with TNF α or A β d/t, and were then fixed after 24h and also immunostained for cofilin-rods using Alexa 647 secondary antibody, a fluorophore that is spectrally well-separated from mRFP. Surprisingly, only about 48% of the rods detected by immunostaining also contained R21Q cofilin-RFP (Fig.15). The reasons for this are not obvious but might be due to: (1) the R21Q cofilin-RFP expression levels might be below the threshold needed to observe rods in many of the cells; this is unlikely due to the fact that rod numbers do not change much when strong or weak promoters are used to drive expression; (2) the presence of the RFP tag on the cofilin might reduce its ability to be incorporated into rods induced by certain stress agents and not others. ATP depletion (Fig.14) induces rods rapidly (complete in 30 min) through mitochondrial produced ROS whereas TNF α or A β d/t stimulates slow rod formation (24 hours) and generates ROS from NADPH oxidase (NOX) and not mitochondria. There might be different ancillary proteins in rods induced by these different agents, some of which are less accommodating to RFP-tagged cofilin. In conclusion, we can

still use R21Q cofilin-RFP as a live-cell reporter for rod formation but need to keep in mind that we might not be observing all the rods induced by certain stresses.

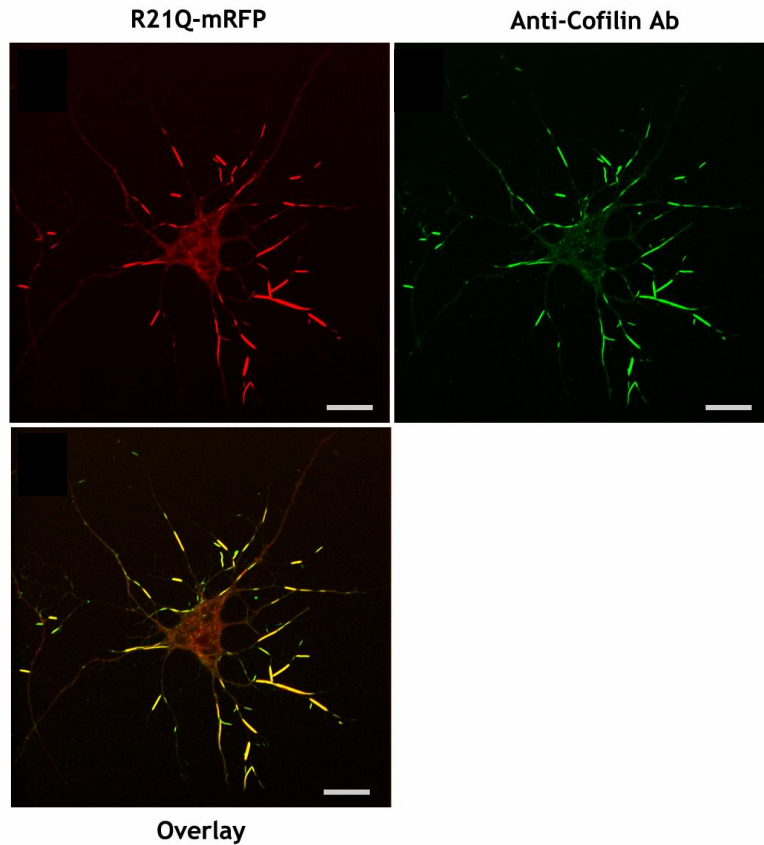


Figure 14. In hippocampal neurons expressing R21Q cofilin-RFP, all rods induced by ATP depletion detected by immunostaining also contained R21Q cofilin-RFP, demonstrating its high fidelity. Rods were induced in neurons infected with virus for expressing R21Q cofilin-RFP 2 days postinfection by ATP depletion with sodium azide and 2-deoxyglucose [Minamide et al., 2000]. After 30 min, cells were fixed and rods were immunostained with 1439 anti-cofilin antibody and an Alexa 488 secondary antibody. R21Q cofilin-RFP incorporates into 100% of rods induced by ATP-depletion. Yellow indicates co-localization in overlay. All scale bars =15 μ m.

[Chi W. Pak, Ph.D. Thesis]

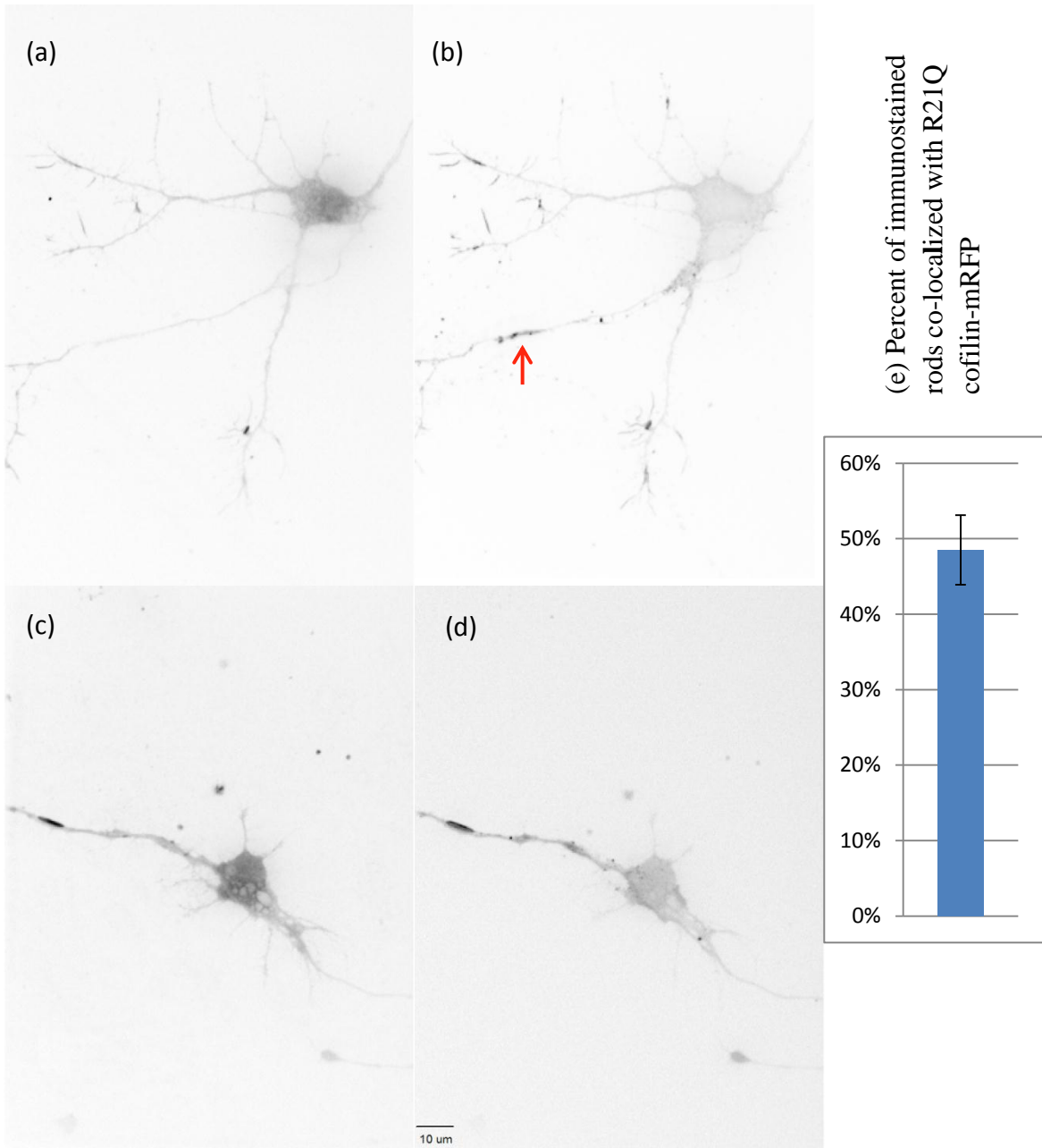


Figure 15. In neurons treated with $TNF\alpha$, only 48 % of the immunostained cofilin-rods co-localized with R21Q cofilin-RFP.

(a)(c) Neurons show the expressed R21Q cofilin-RFP. (b)(d) Neurons show the immunostained cofilin-rod. The arrow indicates an immunostained rod which does not co-localize with R21Q cofilin- RFP.

(e) Percent of immunostained rods co-localized with R21Q cofilin-RFP. About 48% of the rods detected by immunostaining also contained R21Q cofilin- RFP.

The role of lipid rafts in TNF α - and A β d/t- induced rod formation

Lipid rafts are membrane microdomains enriched in cholesterol, sphingolipids and gangliosides, which can segregate specific groups of proteins and thereby provide a hub for cellular signaling and protein trafficking [Callegaro-Filho, et al., 2010]. PIP₂ is enriched on the cytoplasmic face of lipid raft domains. Cofilin can bind to PIP₂ [Moriyama, et al., 1996] and thus might also be concentrated at lipid rafts. Cofilin-actin rods that form in response to TNF α and A β d/t require PrP^c which is concentrated in the exoplasmic face of lipid rafts. Rods likely develop through PrP^c signaling to activate NADPH oxidase. We hypothesize that these lipid raft domains stay small (below some threshold size for cofilin concentration or ROS production) and there is no rod formation, but that TNF α or A β d/t may induce the coalescence of lipid rafts into larger domain. If that reaches a critical size, not only for cofilin, but for the generation of reactive oxygen, it will result in cofilin oxidation leading to rod formation.

To characterize the role of lipid rafts in rod formation downstream of A β d/t and TNF α , we will determine if coalescence of lipid rafts into larger macrodomains is a prerequisite for A β d/t and TNF α -induced rod formation. G_{M1} gangliosides are membrane glycolipids, which are enriched in the exoplasmic face of lipid rafts. CTxB binds specifically to G_{M1} ganglioside [Masco, et al., 1991], and when tagged with a fluorescent dye can be used to identify raft domains.

Cell surface G_M1 labeling was performed by incubating the cells with CTxB Alexa 488 in complete medium for 15 min at 37 °C. We first determined that at 50 ng/mL, CTxB is sufficient to label puncta of G_M1, but not enough to induce a change in aggregation of G_M1 (Fig.16a). When TNF α at 50 ng/mL is added to the culture, we can observe coalescence of CTxB labeled patches over 6 hours (Fig.16b).

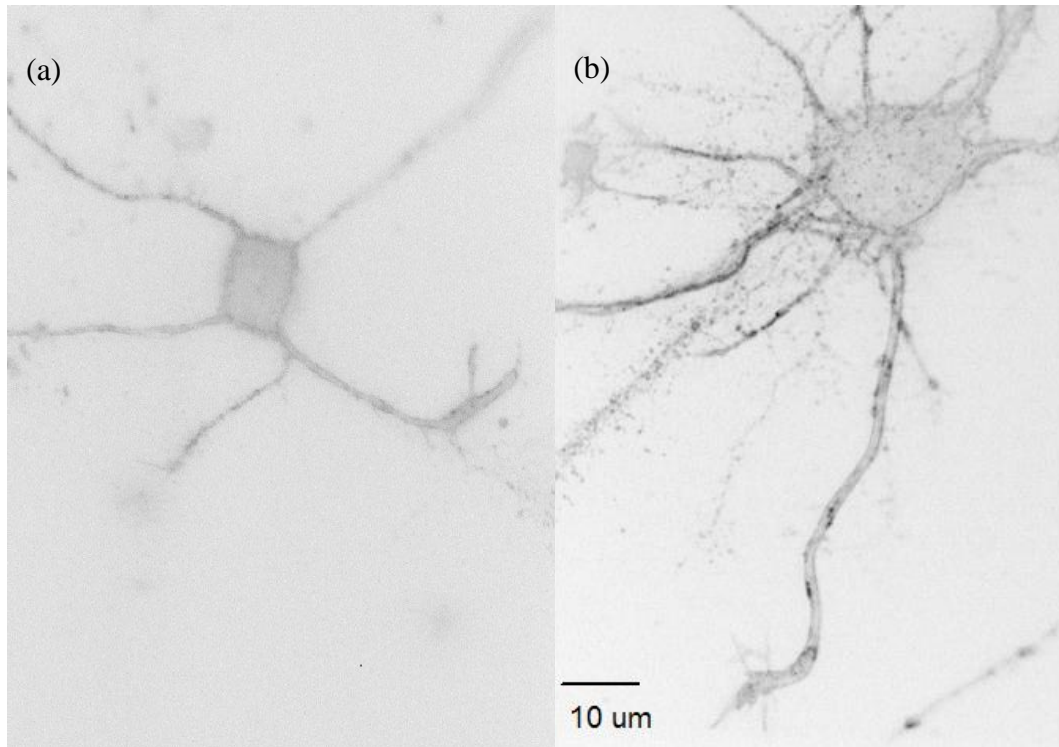


Figure 16. Lipid raft domains in neuronal membranes enlarge upon TNF α treatment.

(a) Inverted fluorescence image of neuron stained with Alexa-CTxB for 15 min.

(b) Inverted fluorescence image of TNF α -treated neuron stained with Alexa-CTxB.

Neurons were stained with CTxB for 15 min after 6 hours treatment with TNF α .

To examine lipid raft coalescence and rod formation simultaneously, hippocampal neurons were infected with adenovirus expressing R21Q cofilin-RFP to follow rod formation. After treatment with A β d/t or TNF α for 24 hours, Alexa 488 CTxB was added to the medium for 15 min. Then neurons were imaged with the spinning disk confocal microscope. To get the time course of raft coalescence and rod formation, time-lapse imaging was performed in 1 hour session in which a total of 12 images were acquired at 5 min intervals to follow formation of new rods.

To determine whether lipid rafts coalesce before or after rod forms, we examined 71 time lapse images of fields of neurons. However, only three new rods formed during the period of observation from all of these movies. We anticipated that raft coalescence would be necessary to signal rod formation. Fig.17 shows the newly formed rods after 30 min during the live cell imaging. However, we observed no coalesced lipid rafts at the sites of newly formed rods.

We then evaluated the total number of rods which co-localized with coalesced lipid raft staining. About 45% of rods formed in TNF α treated neurons expressing R21Q cofilin-RFP showed co-localization with coalesced lipid rafts (Fig.18), suggesting that the coalesced rafts are not required for rod formation but that rods, once formed, can lead to the enlarged lipid raft domains. Because we already know that R21Q cofilin-RFP does not visualize all of the rods induced by TNF α , we decided to immunostain these cultures for total rods using a cofilin antibody and an Alexa 647-secondary that allowed us to look at total rods along with RFP-containing rods

and lipid rafts. We found that 52% of immunostained rods co-localized with coalesced lipid rafts (Fig. 18). Furthermore, only strongly immunostained rods co-localized with the coalesced raft domains (Fig. 19), similar to what we saw initially that led to our doing this study (Fig. 6).

Because we are able to observe only about half the rods that form when we use the R21Q cofilin-RFP for live cell imaging, and these rods do not co-localize with coalesced lipid rafts, it is possible that there are differences in rod structure and formation between rods induced by TNF α which contain the R21Q cofilin RFP and rods formed from the endogenous proteins. Previous studies comparing isolated rods made from cells expressing cofilin-GFP or only endogenous proteins showed some differences in rod stability to reducing agent (DTT) and salt (0.5 M NaCl) with the cofilin-GFP rods being more stable [Minamide, et al., 2010]. Thus, it is possible that the rods that form and incorporate R21Q cofilin-RFP are different in structure or composition from those formed from endogenous proteins. In addition, because we were able to only visualize three new rods forming in the 71 fields of cells that were observed, we cannot rule out the possibility that these were spontaneous rods and not rods induced by TNF α , thus perhaps not requiring lipid-raft mediated NOX signaling for their formation. Since we are unable to visualize all of the rods during their formation, and do not know if the three rods we observed are spontaneous ones or are induced by TNF α , we cannot make a definitive conclusion as to whether lipid raft coalescence precedes or follows TNF α -induced rod formation for rods containing the endogenous cofilin without the R21Q cofilin-RFP tag.

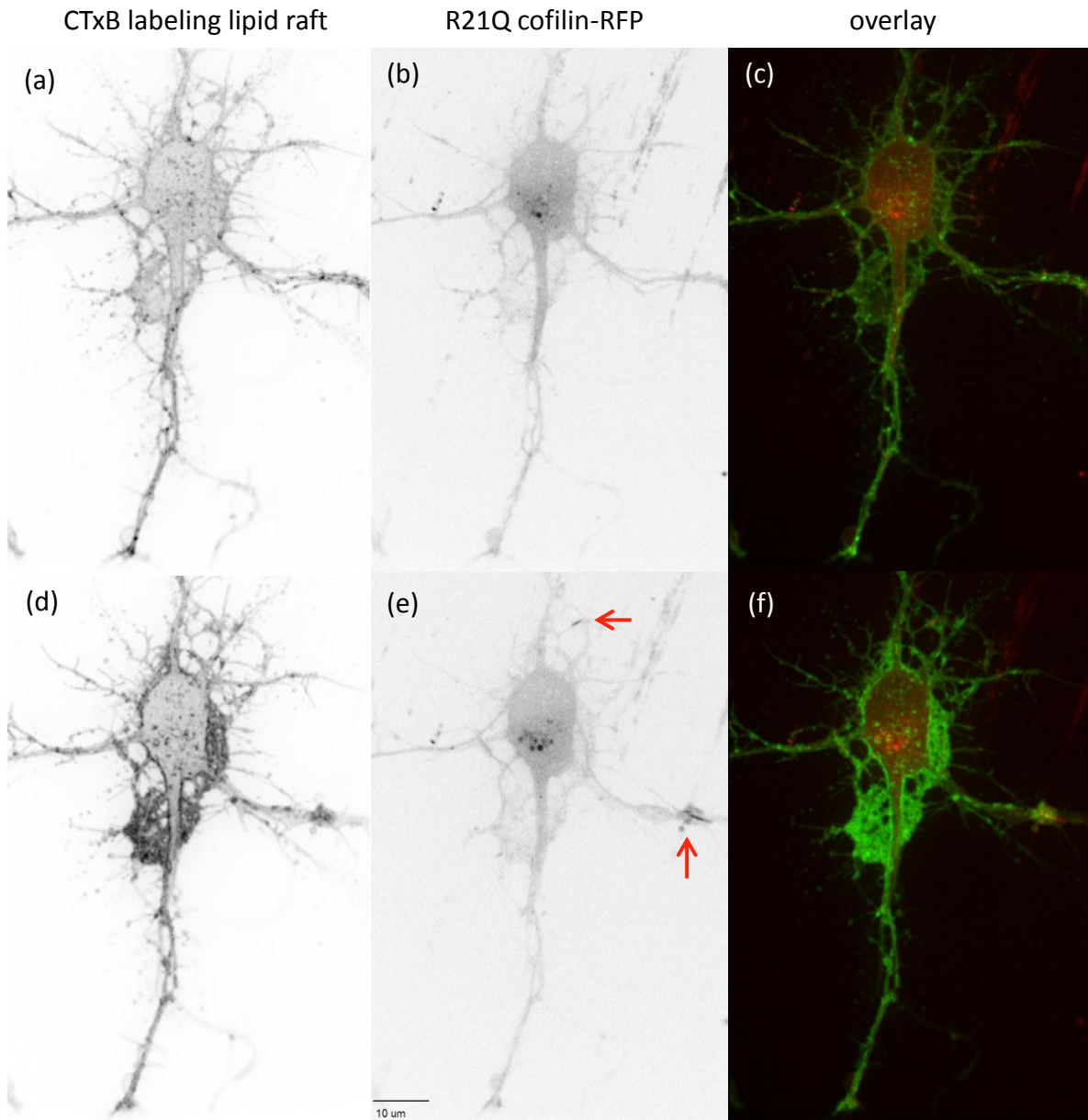


Figure 17. Time lapse images of rod formation.

Neurons were infected with CMV driven R21Q cofilin-RFP. After treatment with TNF α for 20 hours, Alexa 488 CTxB was added for 15 min. Then neurons were taken for live cell imaging for 1 hour at 5 min interval. (a) (d) are inverted images of CTxB staining of lipid raft. (b) (e) are inverted images of expression of R21Q cofilin-RFP. The arrows show the rods that formed after 30 min during the imaging. However, the rods did not co-localize with coalesced lipid raft (c) (f).

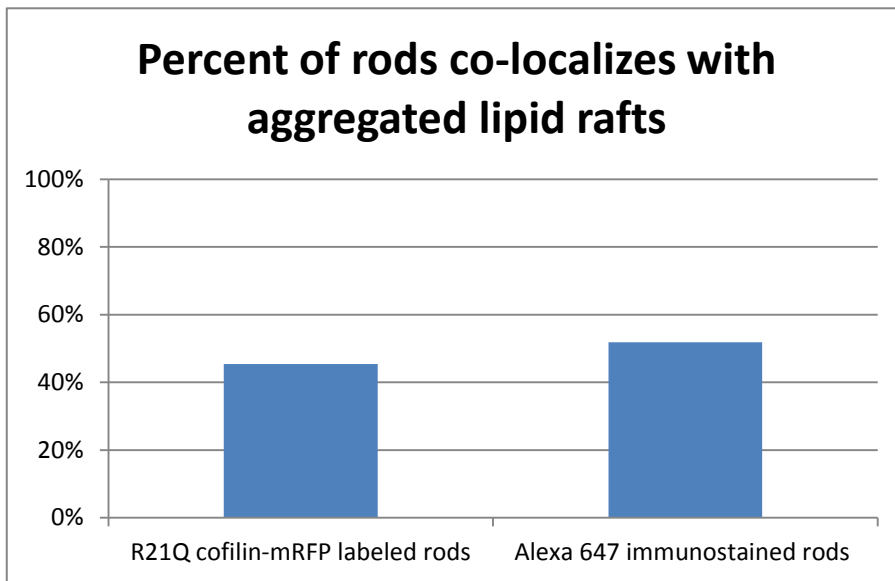


Figure 18. Percent of rods co-localizing with coalesced lipid rafts.

Enhanced CTxB staining is found associated with only 45% of R21Q cofilin-RFP labeled rods and around 52% of Alexa 647 immunostained rods (which should also include all of the R21Q cofilin-RFP rods).

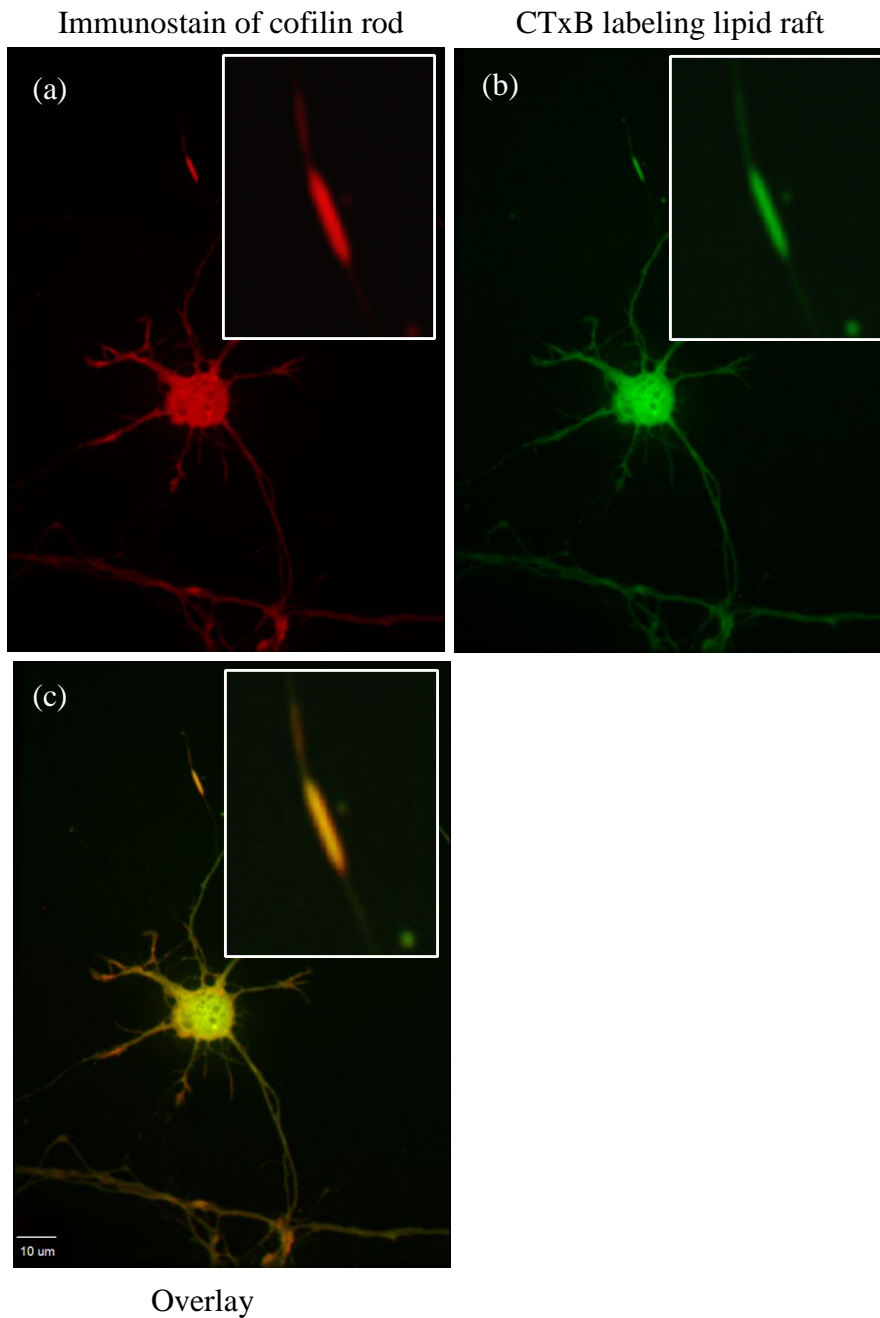


Figure 19. Strongly immunostaining labeled rods seem to form in regions of neurites where raft domains have coalesced. Yellow regions indicate co-localization.

TNF α treatment of R21Q cofilin-RFP expressing neuron induces rod (a) and also region of enhanced Alexa 488-CTxB staining (b) which are enlarged in inset and overlaid in (c).

Future Directions for Research

Overall, this study suggests that R21Q cofilin-RFP can be used as a tag for measuring rod induction in live cells, although it might not labeling all the rods induced by certain stresses. The continued presence of coalesced lipid raft domain is not required for maintaining a rod since we find only about 50% of the rods associated with a coalesced lipid raft. Initial studies by others (Minamide, et al., personal communication) indicate that a cellular prion protein (PrP^c)-dependent signal from A β d/t or TNF α , mediates cofilin activation and oxidation, resulting in formation of cofilin-actin rods. Therefore, rather than looking at the dynamics of the total lipid raft domains by G_M1 gangliosides labeling, we would better focus on localizing PrP^c and characterizing its role in signaling to rod formation. To do this, we will use R21Q cofilin-RFP to follow A β d/t- or TNF α -induced rod formation in neurons expressing PrP^c-GFP to determine if the location of PrP^c-hot spots on membrane corresponds to rod location. We could also co-map PrP^c hot spots to G_M1 ganglioside labeled lipid rafts to determine if these show high co-localization correlation coefficients. We will determine which domain(s) of PrP^c are required for A β d/t or TNF α induced rod formation and if other membrane components are recruited to PrP^c enriched regions in the presence of A β d/t or TNF α .

Others have recently discovered that ursolic acid (UA), a natural triterpene, inhibits rods formation induced by A β d/t or TNF α . Future studies should examine how UA alters the association of PrP^c with membrane binding partners recruited

during A β d/t or TNF α treatment as well as the mechanism by which UA inhibits formation of rods induced by A β d/t or TNF α .

Understanding the PrP^c-mediated signaling pathways to rod formation will likely be important for therapeutic intervention in many neurodegenerative diseases in addition to AD.

References

Bamburg JR. Proteins of the ADF/Cofilin family: Essential regulators of actin dynamics. *Annual Review of Cell and Developmental Biology*, 15,185-230 (1999)

Bamburg JR, Wiggan OP. ADF/cofilin and actin dynamics in disease. *Trends Cell Biol.*, 12, 598-605 (2002)

Bamburg JR, Bloom GS. Cytoskeletal pathologies of Alzheimer Disease. *Cell Motility and the Cytoskeleton*, 66, 635–649 (2009)

Bamburg JR, Bernstein BW, Davis RC, Flynn KC, Goldsberry C, Jensen JR, Maloney MT, Marsden IT, Minamide LS, Pak CW, Shaw AE, Whiteman IT, Wiggan O. ADF/Cofilin-actin rods in neurodegenerative diseases. *Curr AlzheimerRes*, 7, 241-250 (2010)

Bernstein BW, Chen H, Boyle JA, and Bamburg, JR. Formation of actin-ADF/cofilin rods transiently retards decline of mitochondrial potential and ATP in stressed neurons. *Am J Physiol Cell Physiol.*, 5, 828-839 (2006)

Bernstein BW, Shaw AE, Minamide LS, Pak CW, Bamburg JR. Incorporation of cofilin into rods depends on disulfide intermolecular bonds: Implications for Actin Regulation and Neurodegenerative Disease. *J. Neurosci.*, 19, 6670-6681 (2012)

Brewer, GJ, Torricelli, JR, Evege, EK, Price, PJ. Optimized survival of hippocampal neurons in B27 supplemented Neurobasal, a new serum-free medium combination. *J. Neurosci.*, 18, 1217-1229 (1998)

Callegaro-Filho D, Shrestha N, Burdick AE, Haslett PA. A potential role for complement in immune evasion by *Mycobacterium leprae*. *J Drugs Dermatol*, 11, 1373-82 (2010)

Chi W. Pak. Actin dynamics in silico, in waves, and in rods. Ph.D. thesis, Colorado State University (2009)

Cichon J, Sun C, Chen B, Jiang M, Chen XA, Sun Y, Wang Y, Chen G. Cofilin aggregation blocks intracellular trafficking and induces synaptic loss in hippocampal neurons. *J Biol Chem.*, 287, 3919-3929 (2012)

Davis RC, Maloney MT, Minamide LS, Flynn KC, Stonebraker MA, Bamburg JR. Mapping Cofilin-actin rods in stressed hippocampal slices and the role of cdc42 in amyloid β -induced rods. *J Alz Dis*, 18, 35-50 (2009)

Davis RC, Marsden IT, Maloney MT, Minamide LS, Podlisny M, Selkoe D, Bamburg JR. Amyloid beta dimers/trimmers potently induce cofilin-actin rods that are inhibited by maintaining cofilin-phosphorylation. *Mol. Neurodegeneration*, 6:10 (2011)

Garvalov BK, Flynn KC, Neukirchen D, Meyn L, Teusch N, Wu X, Brakebusch C, Bamburg JR, Bradke F. Cdc42 regulates Cofilin during the establishment of neuronal polarity. *J. Neurosci.*, 27, 13117-13129 (2007)

Homma K, Niino Y, Hotta K, Oka K. Ca²⁺ influx through PsX receptors induces actin cytoskeleton reorganization by the formation of Cofilin rods in neurites. *Mol Cell Neurosci.*, 37, 261-270 (2008)

Hotulainen P, Llano O, Smirnov S, Tanhuanpaa K, Faix J, Rivera C, Lappalainen P. Defining mechanisms of actin polymerization and depolymerization during dendritic spine morphogenesis. *J Cell Biol.*, 185, 323-339 (2009)

Jang DH, Han JH, Lee SH, Lee YS, Park H, Lee SH, Kim H, Kaang BK. Cofilin expression induces cofilin-actin rod formation and disrupts synaptic structure and function in *Aplysia* synapses. *Proc Natl Acad Sci USA*, 102, 16072-16077 (2005)

Kim I, W Xu, JC Reed. Cell death and endoplasmic reticulum stress: disease relevance and therapeutic opportunities. *Nat. Rev. Drug Discov.* 7:1013–1030 (2008)

Kuhn TB, Meberg PJ, Brown MD, Bernstein BW, Minamide LS, Jensen JR, Okada K, Soda EA, Bamberg JR. Regulating actin filament dynamics in neuronal growth cones by ADF/cofilin and rho family GTPases. *J. Neurobiol.*, 44, 126-144 (2000)

Lauren J, Gimbel DA, Nygaard HB, Gilbert JW, Strittmatter SM. Cellular prion protein mediates impairment of synaptic plasticity by amyloid-beta oligomers. *Nature*, 457, 1128-1132 (2009)

Maloney MT, Minamide LS, Kinley AW, Boyle JA, Bamberg JR. Beta-secretase-cleaved amyloid precursor protein accumulates at actin inclusions induced in neurons by stress or amyloid beta: a feedforward mechanism for Alzheimer's disease. *J Neurosci*, 25, 11313-11321 (2005)

Masco D, Van de Walle M, Spiegel S. Interaction of ganglioside GM1 with the B subunit of cholera toxin modulates growth and differentiation of neuroblastoma N18 cells. *J Neurosci.*, 11, 2442-52 (1991)

McDonald JM, Savva GM, Brayne C, Welzel AT, Forster G, Shankar GM, Selkoe DJ, Ince PG, Walsh DM; Medical Research Council Cognitive Function and Ageing Study.

The presence of sodium dodecyl sulphate-stable Aβ dimers is strongly associated with Alzheimer-type dementia. *Brain*, 133, 1328-1341 (2010)

Minamide LS, Stregl AS, Boyle JA, Meberg PJ, Bamburg JR. Neurodegenerative stimuli induce persistent ADF/cofilin-actin rods that disrupt distal neurite function. *Nat Cell Biol.*, 2, 628-636 (2000)

Minamide LS, Shaw AE, Sarmiere PD, Wiggan O, Maloney MT, Bernstein BW, Sneider JM, Gonzalez JA, Bamburg JR. Production and use of replication-deficient adenovirus for transgene expression in neurons. *Methods Cell Bio.*, 71, 367-394 (2003)

Minamide LS, Maiti S, Boyle JA, Davis RC, Coppinger JA, Bao Y, Huang TY, Yates J, Bokoch GM, Bamburg JR. Isolation and characterization of cytoplasmic cofilin-actin rods. *J Biol Chem.*, 8, 5450-60 (2010)

Moriyama K, Iida K, Yahara I. Phosphorylation of Ser-3 of cofilin regulates its essential function on actin. *Genes Cells*, 1, 73–86 (1996)

Ohm TG. The dentate gyrus in Alzheimer's disease. *Prog Brain Res*, 163, 723-740 (2007)

Zhao H, Hakala M, Lappalainen P. ADF/cofilin binds phosphoinositides in a multivalent manner to act as a PIP(2)-density sensor. *Biophys J.*, 98, 2327-2336 (2010)